کارگاه های آموزشی مرکز اطلاعات علمی جهاد دانشگاهی

کارگاه آنلاین آشنایی با پایگاه های اطلاعات علمی
بین المللی و
ترفند های جستجو

کارگاه آنلاین
روش تحقیق و مقاله نویسی علوم انسانی

کارگاه آنلاین
پرپوزال نویسی و پایان نامه نویسی

19th International Power System Conference
PSC 2004
98-E-REN-159

A New Approach For Control of Wind Energy Conversion Systems

M. SEDIGHIZADEH[1,2]
PhD Student
m.sedighizadeh@moshanir.com

M. KALANTAR[2]
Associate professor
kalantar@iust.ac.ir

1-Power System Studies Dept.-Power Engineering Consultants-MOSHANIR-Tehran-Iran
2-Electrical Dept.-Iran University of Science and Technology-Narmak-Tehran- 16844,Iran
Tel. +98-21-7808022
Fax. +98-21-7454055

Key words – Adaptive PID Control, RASP1 Wavelets, Wind Energy Conversion System.

Abstract

Grid connected wind energy conversion systems (WECS) present interesting control demands, due to the intrinsic nonlinear characteristics of windmills and electric generators. In this paper a PID control strategy using neural network adaptive RASP1 wavelet for WECS control is proposed. It is based on a single layer feedforward neural networks with hidden nodes of adaptive RASP1 wavelet functions controller and an infinite impulse response (IIR) recurrent structure. The IIR is combined by cascading to the network to provide double local structure resulting in improving speed of learning. This particular neuro PID controller assumes a certain model structure to approximately identify the system dynamics of the unknown plant and generate the control signal. The capability of neuro PID controller to self tuning of an unknown plant is then illustrated through WECS. The results are applied to a typical turbine/generator pair, showing the feasibility of the proposed solution.

1. Introduction

In recent years, an increasing interest on non contaminant energy sources has emerged from the industrial and academic communities. The two main sources of renewable energy, wind and solar, are today economically viable alternatives to conventional electric power generation. Among the interdisciplinary factors contributing to this success are the arrival of new power devices technologies, new circuit topologies and novel control strategies. Environmental and safety demands are soaring a worldwide research effort in these areas.

Wind energy conversion systems (WECS's) are found in standalone, hybrid and grid-connected topologies [1]. Traditionally, wind turbines are linked with induction generators (squirrel cage or wound field), giving a robust, low maintenance system. The main drawback is that the resulting system is highly nonlinear, and thus a

nonlinear control strategy is required to place the system in its optimal generation point. Among others, sliding mode control [2] and fuzzy systems [3] have been proposed as feasible control alternatives.

Many authors [4], [5], have suggested neural networks as power full building blocks for nonlinear control strategies due to their ability to uniformly approximate arbitrary input-output mappings on closed bounded subsets. The idea of neuro control is to first process an identification model that approximates the unknown dynamics of the plant in which the parameters of the neural network are adjusted off-line. The parameters of the proposed predictive controls are then adjusted on-line within a feedback loop based on algebraic computations following the sampled information. The most Famous topologies for this purpose are multiplayer perceptron (MLP) and radial basis function (RBF) networks. The basic structure of a RBF network consists of a single hidden layer of radial nonlinear nodes, centered so that each of them becomes specialized on a particular zone of the input space. The desired response is obtained adjusting the weights connecting the hidden layer with a linear output node, with a supervised or unsupervised training procedure [6].

A neural-network-based structure for WECS's control, It consists of two combined control actions: a supervisory control and an RBF network-based adaptive controller has proposed in [7]. The supervisory control, based on crude bounds of the system's model, drives the system near the equilibrium point. The RBF-based adaptive controller then cancels the tracking error with a user-specified dynamic behavior.

The combination of neural network structures and wavelet transform analysis has been addressed by several authors as an efficient technique for universal function approximation [8] and [9].

This paper proposes a adaptive PID controller using neural network frame RASP1 wavelets. It consist of a single layer feedforward neural networks with hidden nodes of adaptive wavelet functions controller and an infinite impulse response (IIR) recurrent structure. The IIR is combined by cascading to the network to provide double local structure resulting in improving speed of learning**.**

This paper is organized as follows. Section 2 derives the model of the system to be controlled. It consists of a wind turbine of the "propeller" (horizontal axis) type, linked to an induction, wound rotor electric generator. The variable frequency ac power produced is injected to the power grid using a static Kramer drive. The drive's firing angle is used to adjust the generator's resistant torque, allowing control of the turbine's operating point. The resulting open-loop system is highly nonlinear. Section 3 discussed the control strategy proposed and states the adaptive network algorithmic implementation and provides the neuro controller design architecture. Section 4 presents some simulation results. Finally, Section 5 resumes the conclusions.

2. Wind Energy Conversion Systems

2.1. Wind Turbine Characteristics

Before discussing the application of wind turbines for the generation of electrical power, the particular aerodynamic characteristics of windmills need to be analyzed. Here the most common type of wind turbine, that is, the horizontal-axis type, is considered.

The output mechanical power available from a wind turbine is [1].

$$P = 0.5\rho C_p (V_\omega)^3 A \quad (1)$$

Where ρ is the air density, A is the area swept by the blades, and V_ω is the wind speed. C_p is called the "power coefficient," and is given as a nonlinear function of the parameter λ

$$\lambda = \omega R / V_\omega \quad (2)$$

Where R is the radius of the turbine and ω is the rotational speed. Usually C_P is approximated as $C_P = \alpha\lambda + \beta\lambda^2 + \gamma\lambda^3$,where α, β and γ are constructive parameters for a given turbine.

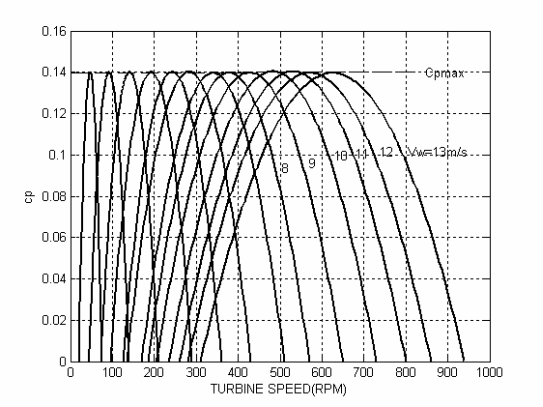

Fig. 1. Power coefficient C_p versus turbine speed

Fig. 1 shows typical C_p versus turbine speed curves, with V_ω as a parameter. It can be seen that $C_{P\max}$, the maximum value for C_P, is a constant for a given turbine. That value, when replaced in (1), gives the maximum output power for a given wind speed. This corresponds to an optimal relationship λ_{opt} between ω and V_ω. The torque developed by the windmill is

$$T_l = 0.5\rho\left(\frac{C_p}{\lambda}\right)(V_\omega)^2\pi R^2 \qquad (3)$$

Fig. 2 shows the torque/speed curves of a typical wind turbine, with V_ω as a parameter. Note that maximum generated power ($C_{P\max}$) points do not coincide with maximum developed torque points.

Superimposed to those curves is the curve of $C_{P\max}$. It can be seen that the maximum C_p (and thus the maximum generated power), and the maximum torque are not obtained at the same speed. Optimal performance is achieved when the turbine operates at the $C_{P\max}$ condition. This will be control objective in this paper.

2.2. Induction Generators and Slip Power Recovery

The vast majority of wind turbines are grid connected through induction generators. There are basically two generator configurations for variable speed constant frequency (VSCF) applications: Cage rotor machines and Wound rotor machines [7].

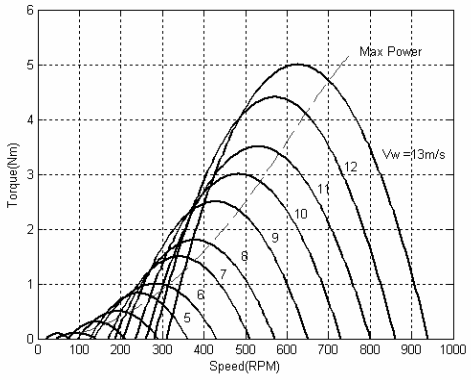

Fig. 2 . Torque/speed curves (solid) of a typical wind turbine. The curve of $C_{P\max}$ is also plotted (dotted).

Fig. 3 depicts a typical wound machine configuration. Varying the firing angle α controls power injection and generator's resistant torque.

Slip power is injected to the AC line using a combination of rectifier and inverter known as a static Kramer drive. Changes on the firing angle of the inverter can control the operation point of the generator, in order to develop a resistant torque that places the turbine in its optimum (maximum generation) point.

The torque developed by the generator/Kramer drive combination is [2].

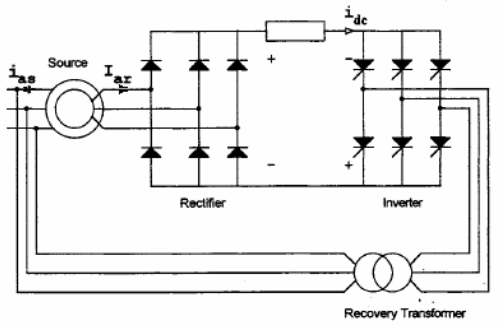

Fig. 3. Slip recovery using a static Kramer drive

$$T_g = \frac{3V^2 sR_{eq}}{\Omega_s[(sR_s + R_{eq})^2 + (s\omega_s L_{ls} + s\omega_s L_{lr})^2]} \qquad (4)$$

Where

$$R_{eq} = \frac{s[n_2^2 sR_b + (n_1|\cos(\alpha)|)^2 R_{s_1} - n_1|\cos(\alpha)|\sqrt{\Gamma}}{((n_2 s) - (n_1|\cos(\alpha)|)^2)} \qquad (5)$$

$$R_b = R_r + 0.55R_f$$

$$\Gamma = 2n_2^2 R_b sR_s + (n_2 sR_s)^2 + n_2^2(s\omega_s L_{ls} + s\omega_s L_{lr})^2 + (n_2 R_b)^2 - [n_1|\cos(\alpha)|(\omega_s L_{ls} + \omega_s L_{lr})^2]$$

and

n_1: transformation rate between rotor and stator wounds;

n_2: transformation rate between the Kramer drive and the AC line;

R_r, R_s, R_f : Rotor ,stator, and dc link resistance;

L_{ls}: stator dispersion inductance;

L_{lr} : rotor dispersion inductance;

α : firing angle;

ω_s :synchronous pulsation;

Ω_s :synchronous machine rotational speed ;

(All values referred to the rotor side).

2.3. Turbine/Generator Model

The dominant dynamics of the whole system (turbine plus generator) are those related to the total moment of inertia. Thus ignoring torsion in the shaft, generator's electric dynamics, and other higher order effects, the approximate system's dynamic model is

$$J\omega^{\bullet} = T_l(\omega, V_\omega) - T_g(\omega, \alpha) \qquad (6)$$

where J is the total moment of inertia. Regarding (3) and (4), system's model becomes

$$\omega^{\bullet} = \frac{1}{J}(0.5\rho(\frac{C_P}{\lambda})(V_\omega)^2 \pi R^2 - \frac{3V^2 sR_{eq}}{\Omega_s[(sR_s + R_{eq})^2 + (s\omega_s L_{ls} + s\omega_s L_{lr})^2]}) \qquad (7)$$

Where R_{eq} depends nonlinearly on the control action $\cos(\alpha)$ according to (5). C_P, λ ,and V_ω also depend on ω in a nonlinear way (2). Moreover, it is well known that certain generator parameters, such as wound resistance, are strongly dependent on factors such as temperature and aging. Thus a nonlinear adaptive control strategy seems very attractive. Its objective is to place the turbine in its maximum generation point, in despite of wind gusts and generator's parameter changes. The situation is sketched on Fig. 4, where T_l and $-T_g$ are plotted for a given V_ω , $\cos(\alpha)$ pair. It must be noted that, for a given wind speed, the turbine operational curve and its optimum generation point are fixed. The equilibrium point ($\omega^{\bullet} = 0$)of the turbine-generator pair is given by the intersection of the T_l and $-T_g$ curves (6). Thus the control strategy proposed consist of changing $\cos(\alpha)$ to produce a generator's resistant pair that settles the turbine on the ω_{opt} , $T_{l(opt)}$ point [7].

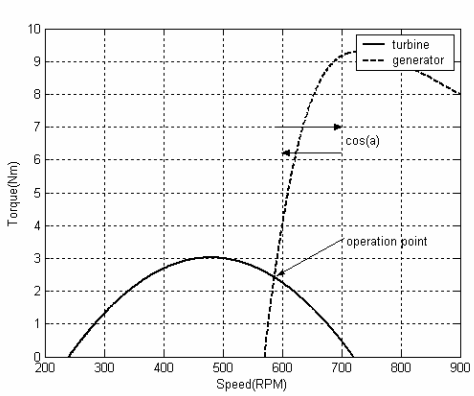

Fig. 4. Control strategy proposed. The firing angle is adjusted so that the turbine's operation point settles to the $C_{P\max}$ condition.

The general form of (6) is $\omega^{\bullet} = h(\omega, \alpha)$, where h is a nonlinear function accounting for the turbine and generator characteristics. The system is usually designed so that the maximum turbine torque correspond to 0.5 to 0.7 of the peak generator torque. The shape of the generator curves in that region allows a simple linearization on the expression for T_g

$$T_g = K_1\omega + K_2\cos(\alpha) \qquad (7)$$

This expression is plotted in dotted lines in Fig. 4. As it can be verified, the proposed approximation is good in the required operation zone. The resulting expression for the whole system is then

$$\omega^{\bullet} = \frac{1}{J}(0.5\rho(\frac{C_P}{\lambda})(V_\omega)^2 \pi R^2 + K_1\omega + K_2\cos(\alpha)) \qquad (8)$$

which has the standard normal form $\omega^{\bullet} = f(\omega) + bu$. here, f is a nonlinear function, b is a constant and $u = \cos(\alpha)$.

3. Proposed Control Strategy

3.1. Structure and alghoritms

Before beginning tracking operation using a neuro network based PID controller , the unknown nonlinear WECS must be identified

according to a certain model. In this particular identification process , the model consist of a neural network topology with the wavelet transform embedded in the hidden units . In cascades with the network is a local infinite impulse response (IIR) block structure as shown in Fig. 5. The IIR synopsis network is used to create a double local network architecture that provides a computationally efficient method of training the system, and accordingly resulting in quick learning, and fast convergence [10]. The algorithm of neural network adaptive wavelets is similar to those in [10] where any desired signal $y(t)$ can be modeled by generalizing a linear combination of a set of RASP1 daughter wavelets $h_{a,b}(t)$,where $h_{a,b}(t)$ are generated by dilaton, *a*, and translation, *b*, from a mother wavelet :

$$h_{a,b}(t) = h(\frac{t-b}{a}) = \frac{\tau}{(\tau^2+1)^2} \quad (9)$$

with the dilaton factor $a > 0$.

That

$$\frac{\partial h_{a,b}(t)}{\partial b} = \frac{1}{a}[\frac{3\tau^2-1}{(\tau^2+1)^3}]$$

and $\tau = \frac{t-b}{a}$

The inversion formula of the wavelet transform cannot be expressed directly by finite neural networks (NN), but can be approximately realized using NN topology with finite hidden units. This is so because most targets are restricted in both the time and frequency domains . Assume that the network output function satisfies the admissibility condition and that the network sufficiently distributes *K* sets of the mother wavelet basis functions, evently portioning the interest region. The approximated signal of the network $\hat{y}(t)$ can be modeled by [11]:

$$\hat{y}(t) = \sum_{i=0}^{M} c_i z(t-i) + \sum_{j=1}^{N} d_j \hat{y}(t-j) v(t) \quad (10)$$

where

$$z(t) = \sum_{k=1}^{K} w_k h_{a_k,b_k}(t) \quad (11)$$

K is the number of wavelets, w_k is the kth weight coefficient . *M* and c_j are the number of feedforward delays and coefficient of the IIR filter, respectively , *N* and d_j are the number of feed back and recursive filter coefficients , respectively. The signals $u(t)$ and $v(t)$ are the input and co-input to the system at time *t*, respectively. Input $v(t)$ is usually kept small for feedback stability purposes.

The neural network parameters a_k, b_k, c_i, w_k and d_j can be optimized in the LMS sense by minimizing a cost function or the energy function , *E* , over all time t.

Thus, $e(t) = y(t) - \hat{y}(t)$ (12)

is a time varying error function at time *t*, where $y(t)$ is the desired (target) response. The energy function is defined by

$$E = \frac{1}{2}\sum_{t=1}^{T} e^2(t) \quad (13)$$

To minimize *E* we may use the method of steepest descent which requires the gradients $\frac{\partial E}{\partial w_k}, \frac{\partial E}{\partial a_k}, \frac{\partial E}{\partial b_k}, \frac{\partial E}{\partial c_i}$ and $\frac{\partial E}{\partial d_j}$ for updating the incremental changes to each particular parameter a_k, b_k, c_i, w_k and d_j respectively. For RASP1 mother wavelet , gradients of *E* are

$$\frac{\partial E}{\partial w_k} = -\sum_{t=1}^{T} u(t)e(t)\sum_{i=0}^{M} c_i h(\tau - i) \quad (14)$$

$$\frac{\partial E}{\partial b_k} = -\sum_{t=1}^{T} u(t)e(t)\sum_{i=0}^{M} c_i w_k \frac{\partial h(\tau-i)}{\partial b_k} \quad (15)$$

$$\frac{\partial E}{\partial a_k} = -\sum_{t=1}^{T} u(t)e(t)\sum_{i=0}^{M} c_i \tau w_k \frac{\partial h(\tau-i)}{\partial b_k} = \tau\frac{\partial E}{\partial b_k} \quad (16)$$

$$\frac{\partial E}{\partial c_i} = -\sum_{t=1}^{T} u(t)e(t)z(t-i) \quad (17)$$

$$\frac{\partial E}{\partial d_j} = -\sum_{t=1}^{T} v(t)e(t)\hat{y}(t-i) \quad (18)$$

where $\tau = \frac{t-b_k}{a_k}$

The incremental changes of each parameter are simply the negative of their gradients,

$$\Delta w = -\frac{\partial E}{\partial w}, \Delta b = -\frac{\partial E}{\partial b}, \Delta a = -\frac{\partial E}{\partial a}, \Delta c = -\frac{\partial E}{\partial c} \text{ ,and } \Delta d = -\frac{\partial E}{\partial d}, \quad (19)$$

thus each coefficient vector $\underline{a}, \underline{w}, \underline{b}, \underline{c}$ and $\underline{d}$ of the network is updated in accordance with the rule

$$\underline{w}(n+1) = \underline{w}(n) + \mu_w \Delta \underline{w} \quad (20)$$

$$\underline{b}(n+1) = \underline{b}(n) + \mu_b \Delta \underline{b} \quad (21)$$

$$\underline{a}(n+1) = \underline{a}(n) + \mu_a \Delta \underline{a} \quad (22)$$

$$\underline{c}(n+1) = \underline{c}(n) + \mu_c \Delta \underline{c} \quad (23)$$

$$\underline{d}(n+1) = \underline{d}(n) + \mu_d \Delta \underline{d} \quad (24)$$

where the subscripted μ values are fixed learning rate parameter

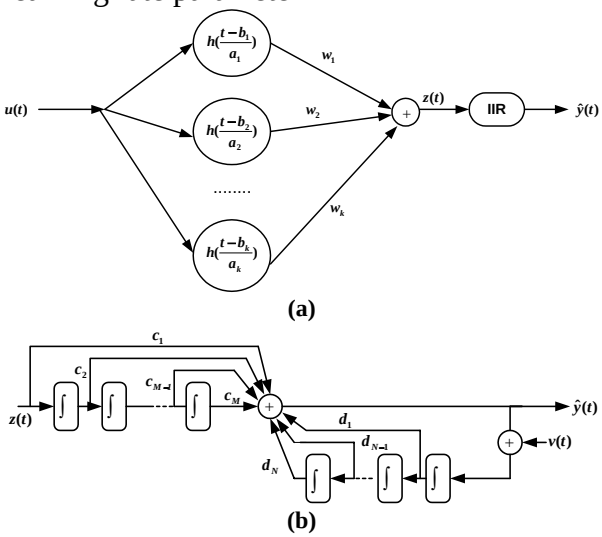

Fig.5. IIR Adaptive wavelet network structure : (a) neural network architecture (b) IIR model

3.2. System Model and PID Controller Design

Consider a general SISO dynamical system similar to (8) be represented by the state equations

$$x^{\bullet} = f(x(t),u(t),t) \quad (25)$$

$$y(t) = g(x(t),t) \quad (26)$$

that in discrete domain rewritten following as

$$x(k+1) = f(x(k),u(k),k) \quad (27)$$
$$y(k) = g(x(k),k)$$

where $x(k) \in R^n$ and $u(k), y(k) \in R$. Further ,let the unknown functions $f, g \in C^1$. The only accessible data are the input *u* and output *y*. It has been [10]that if the linearized system around the equilibrium state is observable, an input-output representation exists which has the form

$$y(k+1) = \varphi(y(k), y(k-1),..., y(k-n+1), u(k), u(k-1),..., u(k-n+1)) \quad (28)$$

i.e. a function $\varphi(.)$ exists that maps $y(k)$ and $u(k)$,and their $n-1$ past values ,into $y(k+1)$. In view of this, a neural network model $\hat{\varphi}$ can be trained to approximate φ over the domain interest. Practically even if an exact model of the plant is available , approximate models are adapted to update the control parameters on-line. The considerations are based on the neural network controller design of the control system . The following alternative model of an unknown plant that can simplify the computation of the control input is described by the equation

$$y(k+1) = \phi(y(k), y(k-1),..., y(k-n+1), u(k) \\ u(k-1),..., u(k-n+1)) + \Gamma(y(k), y(k-1),..., y(k-n+1), \\ u(k), u(k-1),..., u(k-n+1))u(k) \quad (29)$$

For the sake of conciseness and simplicity in the discussion, the complex system representation described above will be generalized for a discrete-time process of dimension 1 of the from

$$y(k+1) = \phi(y(k)) + \Gamma(y(k)).u(k) \quad (30)$$

where $y(k)$ and $u(k)$ denote the input and the output at the *k*th instant of time.

If the nonlinearity terms $\phi(.)$ and $\Gamma(.)$ are known exactly, the required control $u(k)$ for tracking a desired output $r(k+1)$ can be computed at every time instant using the formula

$$u(k) = \frac{r(k+1) - \phi(y(k))}{\Gamma(y(k))} \quad (31)$$

However , if $\phi(.)$ and $\Gamma(.)$ are unknown, the idea is to use the neural network adaptive wavelets model to approximate the system dynamics i.e. ,

$$\hat{y}(k+1) = \hat{\phi}(y(k),\Theta\phi) + \hat{\Gamma}(y(k),\Theta_{\Gamma})u(k) \quad (32)$$

Comparing the model of Eq. (32) with the one of Eq. (10) we can conclude that

$$\hat{\phi}(y(k),\Theta_{\phi}) = \sum_{j=1}^{N} d_j \hat{y}(k-j)v(k) \quad (33)$$

$$\hat{\Gamma}(y(k),\Theta_{\Gamma}) = \sum_{i=0}^{M} c_i z(k-i) \quad (34)$$

After the nonlinearities $\phi(.)$ and $\Gamma(.)$ are approximated by the two distinct neural network functions $\hat{\phi}(.)$ and $\hat{\Gamma}(.)$ with adjustable parameters (including weights w_k , dilations a_k , translations b_k ,IIR feedforward coefficients c_k , IIR feedback coefficients d_k),represented by Θ_{ϕ} and Θ_{Γ} respectively ,the PID control $u(k)$ for tracking a desired output $r(k+1)$ can be obtained from

$$u(k) = u(k-1) + P[\varepsilon(k) - \varepsilon(k-1)] + I\varepsilon(k) + D[\varepsilon(k) - 2\varepsilon(k-1) + \varepsilon(k-2)] \quad (35)$$

where *P*, *I*, and *D* are proportional, integral, and differential gains, $u(k)$ is a plant input at kT, where T is a sampling interval, and

$$\varepsilon(k) = r(k) - y(k) \quad (36)$$

P, *I*, *D* parameters are considered as part of the function of *E* and can be optimized and updated according to the cost function *E* of Eq. (13),

$$P(k) = P(k-1) + \mu_P e(k)\Gamma(k)(\varepsilon(k) - \varepsilon(k-1)) \quad (37)$$

$$I(k) = I(k-1) + \mu_I e(k)\Gamma(k)\varepsilon(k) \quad (38)$$

$$D(k) = D(k-1) + \mu_D e(k)\Gamma(k)(\varepsilon(k) - 2\varepsilon(k-1) + \varepsilon(k-2)) \quad (39)$$

where $\hat{\Gamma}$ comes from Eq. (34), and $\mu(k)$ is the fixed learning rate of each adaptive PID parameter. Figure 6 depicts the block diagram of the resulting network topology based on the PID controller for self-tuning control WECS.

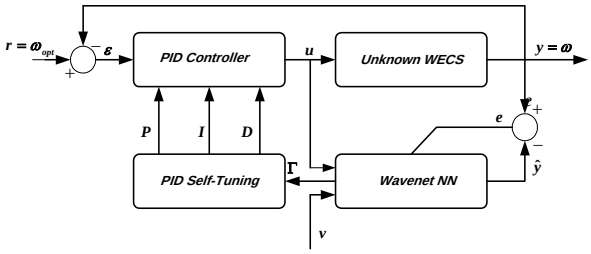

Fig.6. Closed loop block diagram [11]

The optimum shaft rotational speed ω_{opt} is obtained, for each wind speed V_w, and used as a reference for the closed loop. Note that wind speed acts also as a perturbation on the turbine's model. Actually, the turbine is linked with the generator's shaft using a gearbox, which imposes an additional transform relation in the model. Dynamics of this gearbox are considered unknown.

The characteristics of the turbine / generator pair used for the simulations in this article are summarized in [7], but they are considered unknown for the controller. For this reason, the number of wavelets was obtained on a trial-and-error basis.

4. Simulation Results

4.1. Approximation of WECS

In this section , it will be shown through simulations RASP1 mother wavelet basis functions perform their learning ability. Using the data from the WECS extracted from [12], the wavenet network with different size and RASP1 mother wavelets is employed to approximate the WECS data. IIR block structure with feedforward coefficients M=3 and feedback coefficients N=3 is also implemented . Moreover , wavelets are local basis functions that provide less interfering than global ones, leading to a noncomplex dependency in the NN parameters. This section will confirm this idea by providing several observations derived from the results of the MATLAB simulations. Assuming the training data are stationary and sufficiently rich, good performance can usually be achieved with a small learning rate. Thus , all learning rate parameters for weights, dilations , translations , IIR feedforward coefficients , and feedback coefficients are fixed at 0.005 , 0.025 , 0.0250 , 0.01 , and 0.01 , respectively. All initial weights w_k and dilations a_k are set to 0 and 10 , respectively. Note that if the dilation parameters are set too wide , they can cause several overlapping partitions and thus cannot be rallied. Setting a_k too narrow may result in longer convergence.

Initial translation parameters b_k are spaced equally apart throughout the training data to provide non-overlapping partitions throughout the neighboring intervals. Finally , the initial IIR coefficients *c* and *d* should be set so that system has poles inside the unit circle, thus both are set to 0.1.

The number of coefficients for each feedforward and feedback *M* and *N* are both set to 3 as well. The learning epoch will terminate when the desired normalized error of 0.0324 is reached. The following simulations will describe the results of the wavenet network performance employing RASP1 mother wavelets.

Figure 7 and figure 8 illustrates the RASP1 performance. Table .2 provide the numerical values of the experiment, respectively. The results show that *wavenet* employing 36 RASP1 wavelets can reach the error goal of 0.32 in the fastest time among all mother wavelets experimented at 60 iterations. However, again when we oversize the number of wavelets to *K* = 60 and 75, the normalized error starts to oscillate steadily resulting in prolong time consumption to reach the fine

error target. From table. 1, the best number of wavelets to employ in the *wavenet* network for approximation of the WECS model turns out to be 36. Similar to these results have obtained for unknown voice model [11].

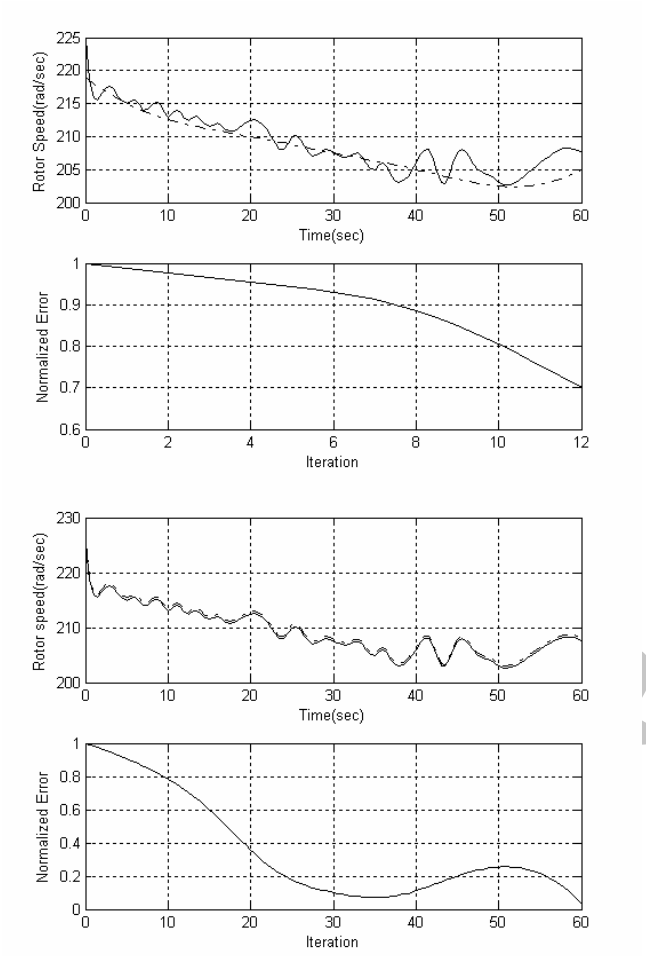

Fig.7. Wavenet simulations with 36 RASP1 waveletsSolid:plant output and Dotted:NN output

4.2. Control

After the identification model is completed, the tracking operation takes command of the neuro process PID control to track the desired setpoint ω_{opt}. The co-input $v(t)$ is set to 0.95.

In Fig. 8 the results of the WECS control using the proposed self-tuning neuro wavenet controller with 36 RASP1 compare with the results of the WECS control using the combined RBF/supervisor control [7]. In this figure, a pseudoaleatory sequence of step-shaped wind gusts is applied to the system. The resulting evolution of the closed loop converges rapidly to the desired optimal rotational speed with simple first-order dynamics. Fig. 9 depicts the turbines developed torque versus rotational speed, for the same input sequence. Superimposed (in dotted line) the turbines characteristic curves are displayed. It can be seen that the torque trajectories of the controlled system converge to points belonging to the maximum torque curve. In Fig. 8. shows that proposed method is better than RBF method [7] regarding simulation accuracy. The proposed controller can be efficiently implemented on digital signal processors.

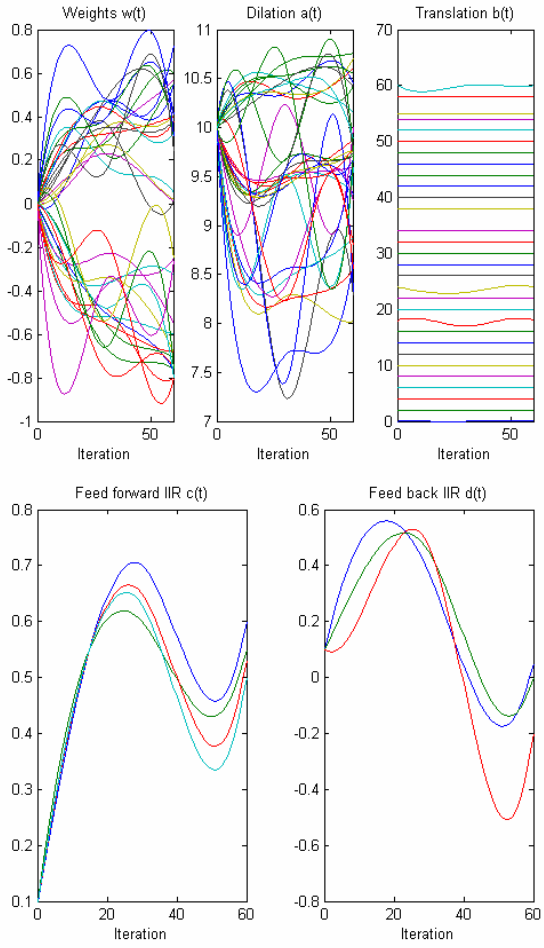

Fig 8. Wavenet Parameter Updates with RASP1 Wavelets

Table 1. Number of Iterations vs. number of RASP1 wavelets Employed

Number of Iterations	*Number 0f Wavelets*							
	9	***15***	***18***	***24***	***36***	***48***	***60***	***75***
Error of 0.85	*17*	*14*	*14*	*14*	*12*	*9*	*9*	*9*
Error of 0.48	*58*	*35*	*20*	*20*	*18*	*15*	*15*	*12*
Error of 0.32	*165*	*73*	*26*	*23*	*21*	*18*	*15*	*15*
Error of 0.15	*300 1*	*128*	*53*	*38*	*27*	*24*	*21*	*60*
Error of 0.05		*205*	*76*	*48*	*55*	*45*	*42*	*oscil late*
Error of 0.04		*232*	*110*	*53*	*57*	*84*	*48*	*oscil late*
Error of 0.032		*310*	*210*	*67*	*60*	*102*	*osci llate*	

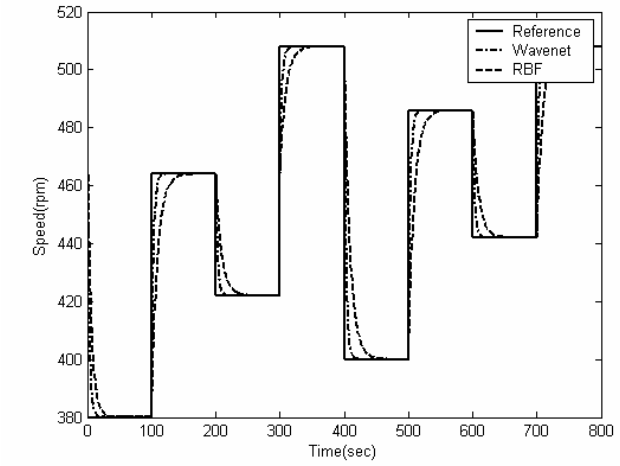

Fig. 8. PID Neuro Wavenet Controller Responses to a pseudoaleatory sequence of wind gusts.

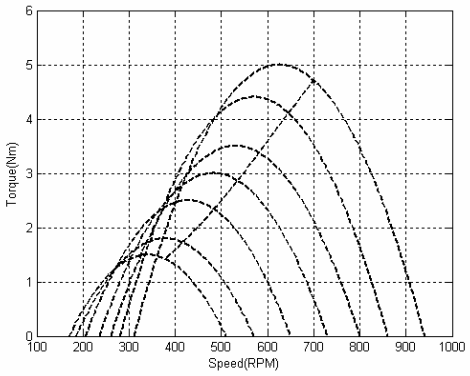

Fig. 9. System response on torque/speed coordinates ,for the same input sequence of fig . 8 .developed torque (points) converges to the maximal torque curve, ensuring optimal operation .

5. Conclusion

This paper discussed the application of wavenet networks in the implementation of adaptive controllers for WECS's. They were proposed to cope with the intrinsic nonlinear behavior of wind turbines/generator. The approach used, based on a single layer feedforward neural networks with hidden nodes of adaptive RASP1 wavelet functions PID controller and an infinite impulse response (IIR) recurrent structure , allowed fast convergence to a simple linear dynamic behavior, even in the presence of parameter changes and model uncertainties. The resulting controller showed to be simple enough to be synthesized using signal processors.

6. References

[1] G. A. Smith, "Power electronics for recovery of wind and solar energy", Wind Eng., Vol. 19, no. 2, 1995

[2] P.Puleston, "Control strategies for wind energy conversion systems", Ph.D. dissertation, Univ. La Plata, Argentina, 1997

[3] P. Simoes, B. K. Bose, and R. J. Spiege, "Fuzzy logic-based intelligent control of a variable speed cage machine wind generation system,", IEEE Trans. Power Electron., Vol. 12, no. 1, Jan. 1997.

[4] F. D. Kanellos, N. D. Hatziargyriou,'A new control scheme for variable speed wind turbine using neural networks",IEEE Power Engineering Society Winter Meeting,2002, Vol.1, 27-31Jan.2002

[5] S. Li, D. C. Wunsch, E. A. O'Hair, "Using neural networks to estimate wind turbine power generation",IEEE Transaction on energy conversion, Vol. 16, No.3, Sept 2001

[6] S. Haykin, Neural Networks, A Comprehensive Foundation. New York: Macmillan, 1994.

[7] M. A. Mayosky, G. I. E. Cancelo,"Direct adaptive control of wind energy conversion systems using gaussian

networks',IEEE Transactions on neural networks, Vol. 10, No. 4,july 1999

[8] Q. Zhang, A. Benveniste," Wavelet networks,"IEEE Trans. Neural Networks, Vol. 3, No.6, Nov.1992

[9] Y. Pati, P. Krishnaprasad,"Analysis and synthesis of feedforward neural networks using discrete affine wavelet transformation ", IEEE Trans. Neural Networks, Vol. 31, No.9, Sept.1992

[10] X. Ye, N. K. Loh,"Dynamic system identification using recurrent radial basis function network,"Proce. American control conf. , Vol. 3,June 1993

[11] G. Lekutai, " Adaptive Self-Tuning Neuro Wavelet Network Controllers ";PhD Thesis, Virginia Polytechnic Institute and State Universitym, 1997

[12] 'Data base of wind characteristics", downloaded from DTU denmark

کارگاه های آموزشی مرکز اطلاعات علمی جهاد دانشگاهی

کارگاه آنلاین آشنایی با پایگاه های اطلاعات علمی بین المللی و ترفند های جستجو

کارگاه آنلاین
روش تحقیق و مقاله نویسی علوم انسانی

کارگاه آنلاین
پروپوزال نویسی و پایان نامه نویسی